Chenchen Lan, Qing Lyu*, XiaoJie Liu, Yana Qie and Shuhui Zhang

Effect of Cl on Softening and Melting Behaviors of BF Burden

https://doi.org/10.1515/htmp-2017-0186
Received December 18, 2017; accepted July 30, 2018

Abstract: The high-temperature simulation tests of softening and melting zone under different $w(Cl^-)$ were carried out, and based on the density functional theory, the influence mechanisms of chlorine on softening and melting behaviors of BF burden were analyzed. The results show that with the increase of $w(Cl^-)$ which bring in by sinter, the softening start temperature and softening end temperature of BF increase, and the softening temperature range becomes small, the melting start temperature increases, the dropping temperature decreases, the melting temperature range becomes small too. The softening and melting zone of BF narrows. With the increase of $w(Cl^-)$, the maximum pressure difference and the comprehensive permeability index both decrease, the permeability of the softening and melting zone enhances. The main reason for the increase of permeability is that the chlorine atom makes the Fe-O bond length increase, the stability of the structure is destroyed, the adsorption capacity of CO molecule on FeO surface is promoted, the reducing speed of FeO increases. Although chlorine can effectively reduce the reduction degradation of sinter in the BF and improve the permeability of the softening and melting zone, the metallurgical enterprises should still eliminate or reduce the chlorine element into the BF.

Keywords: blast furnace, chlorine, softening and melting behavior, adsorption

Introduction

The BF is rapidly developing toward the high-effective and large-scale direction. For the large-scale BF, the requirement for the quality of raw materials is improved. At 400 ~ 600℃, the Fe_2O_3 in sinter is reduced to Fe_3O_4 by the CO, during the process of low temperature phase transformation, the volume expansion produces in sinter with a higher *RDI* (reduction degradation index), which affects the permeability of BF [1–3]. Due to the mineral grade of iron and steel enterprises is more and more low, the harmful elements are becoming more, which affects the quality of sinter seriously. The content of alkali metals in the sinter increase from 0.04% to 0.1%, $RDI_{-3.15}$ increases from 34.2% to 43% [4]. In order to reduce the cost, some enterprises also add some raw materials containing vanadium and titanium to sinter, as a result, the perovskite, which promotes degradation of sinter [5, 6], forms. $RDI_{-3.15}$ of vanadium-titanium sinter is as high as 70–80% [7]. In addition, in order to improve production efficiency, increase the content of H_2 in the BF, reduce the energy consumption, some new technologies were proposed, such as BF gas injection process, oxygen BF process, which makes the reduction potential increase and further strengthens the sinter degradation in the BF lumps [8–10]. $RDI_{-3.15}$ increases about 1.5% ~ 2.5% when H_2 content increases from 0% to 12% [11]. It seriously deteriorates the permeability in the lump zone of BF. In order to improve the metallurgical properties of sinter, the spraying chloride technology on the surface of sinter is applied to reduce *RDI*. However the technology makes the $w(Cl^-)$ has a substantial increase. At the same time, coal and coke contain Cl elements, and Japan proposed to injection waste plastics via BF tuyere, which in the high temperature region the Cl^- are released in different forms [12–15]. The results show that the different forms of chloride have great influences on metallurgical properties of BF burden, among which Cl plays a major role [16].

The influences of Cl on BF smelting have been studied extensively by scientific research workers. The experimental results indicated that spraying chloride solution can effectively decrease the *RDI* of sinter and improve the permeability in the lumpy zone of BF [17, 18]. However, most of them focused on researching the metallurgical properties of sinter at the low temperature. Cl enters the BF with burden and reaches the softening and melting zone of BF. This will certainly have a significant effect on the softening and melting property of

***Corresponding author: Qing Lyu,** College of Metallurgy & Energy, North China University of Science and Technology, Tangshan 063009, China, E-mail: lq@ncst.edu.cn
Chenchen Lan, School of Metallurgy, Northeastern University, Shenyang 110819, China, E-mail: 15081586028@163.com
XiaoJie Liu: E-mail: 315173781@qq.com, **Yana Qie:** E-mail: 461434073@qq.com, **Shuhui Zhang:** E-mail: zhangshuhui@ncst.edu.cn, College of Metallurgy & Energy, North China University of Science and Technology, Tangshan 063009, China

BF burden. The softening and melting property of burden plays a vital role in BF production, which directly affects the coke rate, the secondly distribution of BF gas flow, permeability and the other important parameters. Therefore, studying the influences of Cl on the softening and melting behaviors in BF, and mastering the influence laws and mechanisms are especially important, it can provide technical and theoretical support for BF production.

Test program

The mixed burden which was used in the tests consisted of pellet, sinter and lump ore, and all the burden was produced in the industry process. The burden structure was shown in Table 1.

Table 1: Burden structure.

Burden	Sinter	Pellet	Lump ore	Basicity
Proportion/%	64.55	32.52	2.93	1.47

After the sinter, pellet, lump ore and coke were crashed and screened, the appropriate particle of sinter, pellet and lump ore was 6.3 ~ 10 mm while that of coke was 10 ~ 16 mm. Then the burden was dried for 2 h at 105 ± 5℃. Then put it in the desiccator for using. The mixed burden with different $w(Cl^-)$ was obtained by spraying $CaCl_2$ solution on the surface of sinter, $w(Cl^-)$ was the ratio between the quality of $CaCl_2$ and sinter, it was 0, 4×10^{-4} and 8×10^{-4}, respectively. Then the sinter that has been sprayed $CaCl_2$ solution was dried for 2 h at 105 ± 5℃.

The schematic of the experimental apparatus during the test was shown in Figure 1. The high temperature test could reach 1600℃, which was supplied heat by 6 $MoSi_2$ heating bodies. The size of the corundum reaction tube was $\Phi80\times5\times800$ mm. The temperature was controlled by DWK-702 temperature controller.

In the graphite crucible, the coke is put for 20 mm firstly, then the mixed burden is put for 50 mm, finally the coke is put for 20 mm again. The tests were completed in load of 1 kg/cm^2. Heating up rate was 10℃/min below 900℃, and 5℃/min from 900℃ to the end of test (the first iron dropping down). Gas flow was 5 L/min of N_2, below 500℃ and 15 L/min of reducing gas (N_2:CO = 7:3) over 500℃. The layer thickness, pressure drop and temperature were all recorded automatically by computer. The specific test parameters are shown in Table 2.

The permeability index which reflects the total pressure difference across the softening and melting zone was expressed by S and can be calculated by eq. (1):

$$S=\int_{T_s}^{T_d}(\Delta P_T-\Delta P_S)dT \tag{1}$$

where ΔP_T was the pressure difference at the temperature of T, ΔP_S was the pressure difference at the temperature of melting start temperature(Ts).

The specific test schemes and results are shown in Table 3

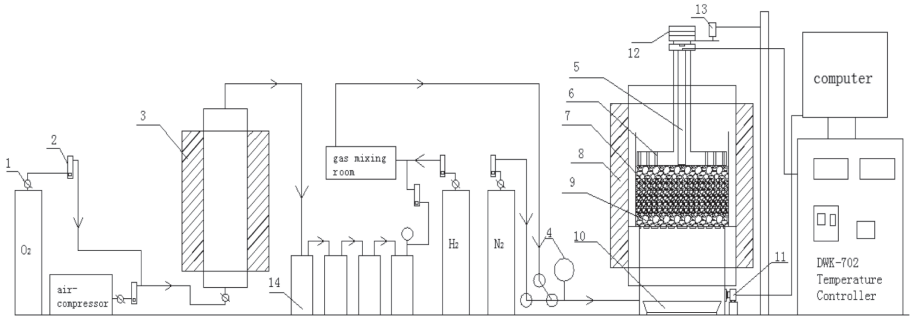

1-gas valve 2-gas flow-meter 3-gas-producing furnace 4-piezometer 5-platinum-rhodium thermocouple 6-compression bar 7-Iron-bearing feed 8-$MoSi_2$ high temperature furnace 9-coke 10-receiving disc 11-camera 12-pressure device 13-displacement sensor 14-gas-washing bottle

Figure 1: Structure of experimental equipment.
1-gas valve 2-gas flow-meter 3-gas-producing furnace 4-piezometer 5-platinum-rhodium thermocouple 6-compression bar 7-Iron-bearing feed 8-$MoSi_2$ high temperature furnace 9-coke 10-receiving disc 11-camera 12-pressure device 13-displacement sensor 14-gas-washing bottle

Table 2: Test parameters of softing and melting behavior of burden.

Parameters	Symbol	Unit	Parameters	Symbol	Unit
Softening start temperature	$T_{10\%}$	℃	Softening interval	$\Delta T_a = T_{40\%} - T_{10\%}$	℃
Softening ending temperature	$T_{40\%}$	℃	Melting interval	$\Delta T_{ds} = T_d - T_s$	℃
Melting start temperature	T_S	℃	Maximum pressure difference	ΔP_{max}	kPa
Dripping temperature	T_d	℃	Permeability index	S	kPa℃

Table 3: Test schemes and results.

Number	$w(Cl^-)$	$T_{10\%}$/℃	$T_{40\%}$/℃	ΔT_1/℃	T_s/℃	T_d/℃	ΔT_{dS}/℃	ΔP_{max}/kPa	S/kPa℃
1#	0	1210	1380	170	1283	1457	160	15.72	1862
2#	4×10^{-4}	1236	1394	158	1288	1445	145	15.04	1406
3#	8×10^{-4}	1238	1400	162	1307	1443	132	13.34	1198

Effect of Cl on softening and melting behaviors of BF burden

Figure 2 shows the $T_{10\%}$ and $T_{40\%}$ with different $w(Cl^-)$. It can be seen from Figure 2, with increasing of $w(Cl^-)$ in softening and melting zone of BF, $T_{10\%}$ and $T_{40\%}$ both increase. When $w(Cl^-)$ increases from 0 to 4×10^{-4}, $T_{10\%}$ increases from 1210℃ to 1380℃, $T_{40\%}$ increases from 1380℃ to 1394℃, and ΔT_1 decreases from 170℃ to 158℃, ΔT_1 decreases by 12℃. When $w(Cl^-)$ continues to increase to 8×10^{-4}, $T_{10\%}$ is 1238℃ and $T_{40\%}$ is 1400℃, the changes in $T_{10\%}$ and $T_{40\%}$ are small. ΔT_1 is 162℃, ΔT_1 has a small increase. Figure 3 shows the T_S and T_d with different $w(Cl^-)$. It can be seen that, with increasing of $w(Cl^-)$ in softening and melting zone of BF, the T_s increases while the T_d decreases. When $w(Cl^-)$ increases from 0 to 8×10^{-4}, T_S increases from 1283℃ to 1307℃, T_d decreases from 1457℃ to 1443℃, and ΔT_{ds} becomes small from 160℃ to 132℃, the ΔT_{ds} decreases by 28℃. This indicates that the softening and melting zone of BF narrows and the permeability improves with increasing of $w(Cl^-)$.

Figure 4 shows the ΔP_{max} with different $w(Cl^-)$. With increasing of $w(Cl^-)$ in softening and melting zone of BF, ΔP_{max} decreases. The ΔP_{max} of 1# is 15.72kPa which is maximum. The secondly is 2#, the ΔP_{max} is 15.04kPa. And the ΔP_{max} of 3# is minimum, it is 13.04kPa.

Figure 5 shows the S with different $w(Cl^-)$. It can be seen from Figure 5, with increasing of $w(Cl^-)$ of softening and melting zone in BF, S decreases. When $w(Cl^-)$ increases from 0 to 4×10^{-4}, S decreases from 1862kPa℃ to 1406kPa℃, S decreases by 456kPa℃. When $w(Cl^-)$ is 8×10^{-4}, S is 1198 kPa℃, it has 208kPa℃ discrepancy, the decrease of S reduces. The comprehensive permeability improves, which is conducive to the BF operation.

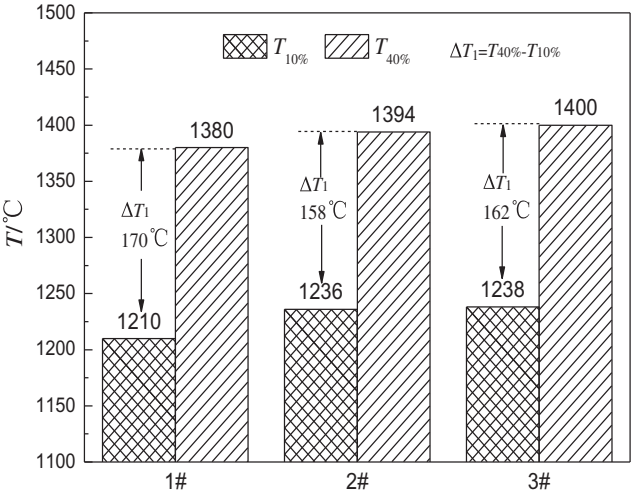

Figure 2: $T_{10\%}$ and $T_{40\%}$ with different $w(Cl^-)$.

Mechanism analysis

Influence mechanism of Cl on the softening behavior of BF burden

The main reason of softening behavior in softening and melting zone is the gradual reduction from Fe_2O_3 to FeO. The FeO forms some low melting point materials. With increasing of temperature, the burden gradually softens. The extensive researches have been done about the effects of Cl on sinter reduction. Sun Yanqin [19] has used density functional theory to calculate the adsorption characteristics of Cl on the surface of iron oxides. It has been determined that Cl could make the Fe-O bond length shorter, the bond energy increases, so that the Fe_2O_3 structure became compact and stable. Zhang

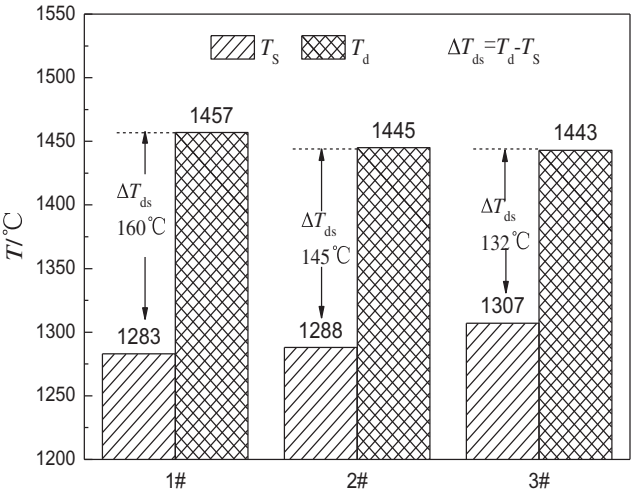

Figure 3: T_S and T_d with different $w(Cl^-)$.

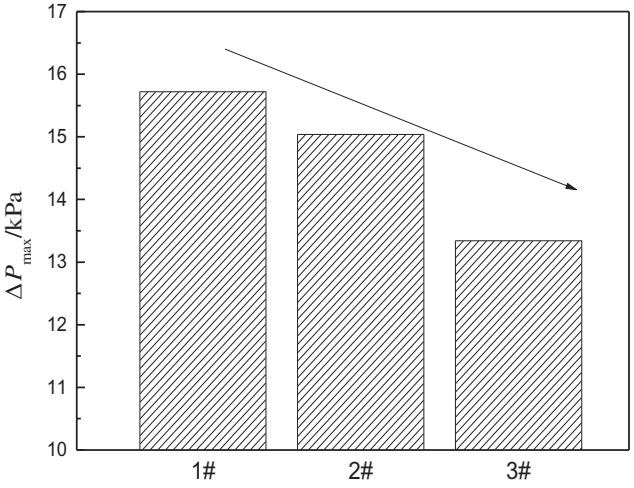

Figure 4: ΔP_{max} with different $w(Cl^-)$.

Jianliang [17] has used infrared spectroscopy to detect the sinter which immersed in 4% $CaCl_2$ solution. The research showed that the Cl reacted with the Fe_2O_3 surface, which made the Fe-O bond increase. It has studied the influence of Cl on sinter reducibility by high temperature simulation tests, the research showed that the reduction degree of sinter decreases with the increase of $w(Cl^-)$ [17].

From the above conclusions, the process of Fe_2O_3 reduction to FeO is inhibited by the function of Cl, the amount of FeO in softening and melting zone decreases, the low melting point compounds decrease, $T_{10\%}$ and $T_{40\%}$ increase. T_s depends on the amount of FeO in primary slag. Therefore, the Cl also makes T_s increase.

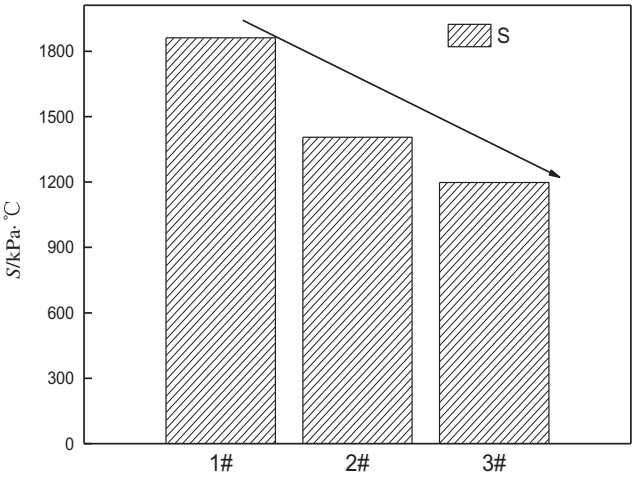

Figure 5: *S* with different $w(Cl^-)$ of sinter.

Influence mechanism of Cl on the melting behavior of BF burden

The melting behavior mainly depends on the reduction of FeO. The Cl in melting zone adsorbs on the surface of the FeO lattice, which affects the reduction of FeO. Therefore, the density functional theory was used to study on the effect of Cl on the reduction of FeO.

All the calculations were performed by the Cambridge Serial Total Energy Package (CASTEP) plane-wave code [20]. The exchange and correlation interactions were modeled using the PW91 of functional within the generalized gradient approximation (GGA). The plane-wave basis set was used to expand the electronic wave function. In order to reduce the number of plane-wave basis sets, the interaction potential between ions and valence electrons was described by using the ultrasoft pseudopotential [21], the fast Fourier transform method was adopted to realize the physical quantity fast conversion between real space and reciprocal space. In the reciprocal k space, the calculation accuracy could be adjusted by changing the plane-wave truncation energy. In the Brillouin zone, when the charge density and the total energy of the system were calculated, Monkhorst-Pack scheme was used to select k space grid points [22].

The wave functions of the valence electrons were expanded using a plane-wave basis set within a specified cutoff energy of 340 eV. The following convergence criteria for the structure optimization and energy calculation were set: (a) a self-consistent field (SCF) tolerance of 2.0×10^{-6} eV/atom, (b) a total energy difference tolerance of 1.0×10^{-5} eV/atom, (c) a maximum force tolerance of 3×10^{-3} eV/nm, and (d) a maximum displacement tolerance of 1×10^{-4} nm.

FeO is a NaCl type oxide, with the face centered cubic structure, and the FeO unit cell (a = 0.4332 nm) is showed in Figure 6. According to the parameters mentioned above, the geometry optimization of FeO structure is carried out. The calculated lattice constant of bulk FeO is 0.4347 nm, which is a little larger than the experimental value (0.4332 nm), the error is 0.347% that is allowed, the adopted calculation method and the setting value of the calculation parameters are reliable. Spin polarization has effects on the adsorption energy and geometry optimization results, therefore the calculation process takes into account spin polarization.

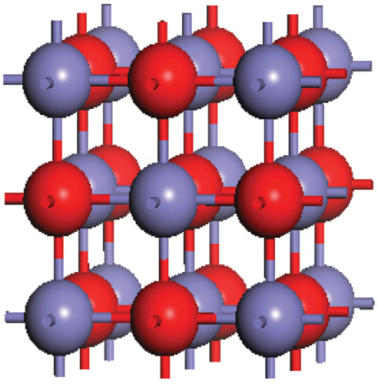

Figure 6: Crystal structure of FeO.

It has been concluded that the surface of FeO(100) is more stable and symmetrical than other surface terminations [23]. Therefore, all of our calculations were based on the FeO(100) surface. The FeO(100) surface was modeled using periodic three-layer slab models, and each slab was separated by a 1.2 nm vacuum layer to minimize interactions between the slabs. During the geometry optimization, the top layer was allowed to relax, whereas the bottom two layers were fixed. The FeO surface was modeled with three surface configurations, using $4 \times 4 \times 1$ k-point Monkhorst-Pack mesh for the (2×2) FeO supercells, respectively.

The binding energy (E_{bind}) of an adatom on the FeO (100) surface was calculated according to eq. (2):

$$E_{bind} = E_{A+S} - (E_s + E_A) \tag{2}$$

where:

E_{A+S} —the calculated total energies of the FeO (100) surface with an adatom,

E_S —the calculated total energies of the clean FeO surface,

E_A — the calculated by placing a single adatom on the center of a cubic.

When the Cl atom was adsorbed on the FeO (100) surface, there are four adsorption sites on the FeO (100) surface including Fe top site, O top site, hollow site, and bridge site, as shown in Figure 7. The adsorption energy was shown in Table 4.

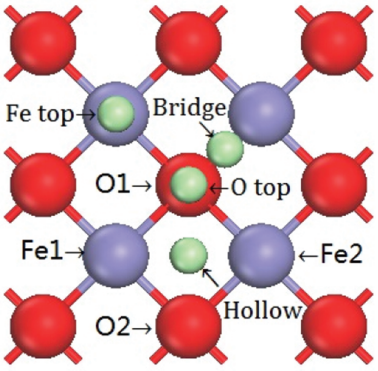

Figure 7: Different adsorption sites of Cl atom.

It can be seen from Table 4, after the Cl atom adsorbs on the FeO(100) surface, the stability order of the adsorption system is determined by the adsorption energy. The order is O top site < bridge site < Fe top site < hollow site. The hollow site is the most stable, and the adsorption energy is −321.20 kJ/mol. The Fe-O bond length is 0.217 nm before the Cl atom adsorbs. After the Cl atom adsorbsathollowsite, the bond length of Fe1–O2、Fe1–O2、Fe2–O1、Fe2–O2 which around the Cl atom are 0.2230 nm, 0.2244 nm, 0.2234 nm, 0.2245 nm, respectively. They all increase with a different extent. Thus it may be known, due to the Cl atom adsorption on the FeO (100) surface, the Fe-O bonds length increase, and the stability of the structure is destroyed.

In order to study on the effect of Cl on FeO reduction by CO, the adsorption energy of CO on O top site in the FeO(100) surface and the bonding state of CO molecule with the surface O atom were calculated in the case of Cl atom adsorption and no Cl atom adsorption, respectively.

The C atom of the CO molecule is adsorbed on the O top site, and the CO molecule is perpendicular to the FeO (100) surface. The conformation A is the adsorption of CO on FeO(100) surfaces without Cl atom, and on the contrary for the configuration B. A and B, the two stable adsorption configurations of (2×2)FeO(100) surface, are obtained by optimization calculation, as shown in the Figure 8.

Table 4: Adsorption energy and configuration parameters of adsorption of Cl on FeO(100).

Adsorption sites	Fe top	Bridge	O top	Hollow
E_{bind}/ (kJ/mol)	−319.366	−314.060	−204.356	−321.200

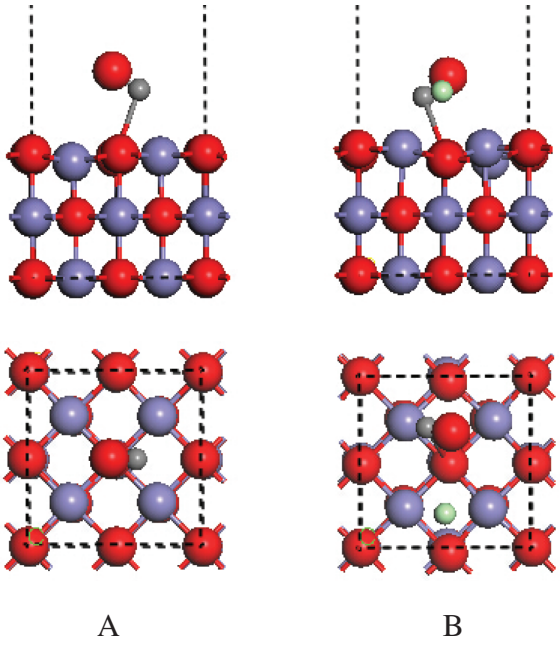

Figure 8: Adsorption configuration of CO adsorption on FeO(100).

It can be seen from the calculation that the adsorption energy of A is −15.447kJ/mol, and the adsorption energy of B is −47.731 kJ/mol. The stability of the configuration A is stronger than the configuration B. As a result, the Cl atom is conducive to reduction of FeO.

There is a large amount of FeO in the primary slag in melt interval of softening and melting zone, and the Cl promotes the reduction of FeO as soon as possible, which makes the T_d decrease. At the same time, due to the reduction of FeO, the amount of primary slag in melting zone decreases and the permeability of the melting zone improves.

Discussion of the use of Cl in BF

With the extensive application of Cl in metallurgical enterprises, the harms to BF smelting have become more and more prominent. With the burden of chloride into the BF through a series of chemical reactions, a part of chloride into BF slag and discharge with BF slag [24–26], some are recycled enrichment in the form of chlorides in the BF [12, 27], most of the Cl with the BF gas discharged into the gas pipeline, the follow-up equipments of BF are corrode, the serious will force BF wind off or stop production to maintenance [28, 29]. The results show that Cl can degrade the high-temperature metallurgical properties of coke and reduce its high-temperature metallurgical strength [30, 31], thus affecting the gas permeability and liquid permeability of BF softening and melting zone, and becoming the restricted link of BF strengthening smelting. At the same time, some of the Cl in the BF exist under the form of HCl gas, which has a strong corrosive effect on the BF refractory, and affects the longevity of the BF [32]. Therefore, although the Cl can effectively reduce the sinter reduction degradation in BF and improve the permeability of the softening and melting zone of BF, metallurgical enterprises should still eliminate or reduce the Cl elements into the BF. It is the fundamental measures to solve the sinter reduction degradation that establishing a comprehensive evaluation standard of Cl, comprehensively evaluating the influence of Cl on BF smelting, and seeking effective alternatives or new technological measures.

Conclusions

1. With increasing of $w(Cl^-)$ in the softening and melting zone of BF, $T_{10\%}$ and $T_{40\%}$ both increase, the temperature range of softening becomes small, T_s increases, T_d decreases, and the temperature range of melting becomes small too. Therefore, the softening and melting zone of BF narrows.
2. With increasing of $w(Cl^-)$ in the softening and melting zone, ΔP_{max} and S both decreases, and the permeability of softening and melting zone enhances.
3. Cl makes the Fe-O bond length increase, which reduces the stability of the FeO crystal structure. The adsorption of Cl promotes the adsorption of CO molecule on FeO (100) surface, and the reduction of FeO is promoted.
4. Although the Cl is beneficial to improve the permeability of the lump zone and softening and melting zone in BF, but it is harmful to the BF refractory, metallurgical properties of coke, gas pipeline and so on. Therefore, it is suggested to reduce the Cl content in BF.

Acknowledgements: The authors are grateful for financial support from the Key Program of the National Natural Science Foundation of China (U1360205), the North China University of Science and Technology Distinguished Youth Scholars Fund (JP201508).

References

[1] Y.H. Yu, G.S. Feng and D.X. Su, J. Iron Steel Res., 15 (2008) 9–12.
[2] S.L. Wu, X.Q. Liu, Q. Zhou, J. Xu and C.S. Liu, J. Iron Steel Res., 18 (2011) 20–24.
[3] H.P. Pimenta and V. Seshadri, Ironmaking Steelmaking, 29 (2002) 169–174.
[4] Z.W. Yan, X.Y. Li, Z.J. Liu, J.L. Zhang, Y. Xiang, B. Gao and H.S. Zhang, Sintering. Pelletizing, 41 (2016) 1–5.
[5] W.S. Wang, Q. Lv, F.M. Li, Y.C. Jin and B.S. Hu, Sintering Pelletizing, 31 (2006) 11–15.
[6] Q. Gan, M.G. He and Q. He, Sintering Pelletizing, 34 (2009) 14–19.
[7] J.G. Shan, Z.G. Ren and S.G. Liu, Sintering Pelletizing, 20 (1995) 1–6.
[8] M. Taichi, K. Takeyuki and K. Eiki, ISIJ. Int., 55 (2015) 1181–1187.
[9] T. Murakami, Y. Kamiya and T. Kodaira, ISIJ. Int., 52 (2012) 14471453.
[10] L. Mu, X. Jiang, Q.J. Gao and F.M. Shen, J. Iron Steel Res., 19 (2012) 6–10.
[11] F.M. Shen, X. Jiang, G. Wei, H.Y. Zheng and L. Mu, China Metall., 24 (2014) 2–5.
[12] C.C. Lan, S.H. Zhang, Q. Lyu, F.M. Li and L.H. Zhang, Iron Steel Vanadium Titanium, 37 (2016) 112–118.
[13] M. Okeda, M. Hasegawa and M. Iwase, Metall. Mater. Trans. B, 42B (2011) 281–290.
[14] M. Makoto and M. Kazuki, ISIJ. Int., 10 (2002) 1065–1070.
[15] H. Taro and M. Kazuki, ISIJ. Int., 10 (2000) 943–948.
[16] C.C. Lan, S.H. Zhang, X.J. Liu, Q. Lyu and B.Q. Wu, J. T. Univ. Tech., 47 (2016) 5–10.
[17] X. Zhang, J.L. Zhang, Z.W. Hu, H.B. Zou and H.W. Guo, J. Iron Steel Res., 17 (2010) 7–12.
[18] X.J. Liu, S.H. Zhang, Y.Q. Sun, Q. Lyu and Z.F. Chen, Iron Steel Vanadium Titanium, 35 (2014) 74–77.
[19] Y.Q. Sun, Q. Lyu, X.Y. Wan, S.H. Zhang and J.M. Zhang, J. Iron Steel Res., 21 (2014) 11–16.
[20] D. Vanderbilt, Phys. Rev. B, 41 (1990) 7892–7895.
[21] H. Monkhorst and J.D. Pack, Phys. Rev. B, 13 (1976) 5188–5192.
[22] L.L. Wang, W.K. Chen, C.H. Lu and Y. Li, Chin. J. Catal., 30 (2009) 560–564.
[23] P. Hohenberg and W. Kohn, Phys. Rev. B, 136 (1964) 864–871.
[24] S.H. Zhang, C.C. Lan, Q. Lyu, Y.Q. Sun and Y.N. Qie, Iron Steel, 51 (2016) 17–21.
[25] Y.K. Fu and X.S. Tang, J. A. Univ. Tech., 29 (2012) 198–201.
[26] B.S. Hu, Y.L. Gui, K. Lyu and J.J. Mi, J. Iron Steel Res., 25 (2013) 23–25.
[27] J.L. Zhang, C. Wang, H.B. Zuo, K.X. Jiao and Z.Y. Wang, Iron Steel, 50 (2015) 1–7.
[28] D.H. Dang and L.S. Gao, Metall. Power, 6 (2007) 24–29.
[29] S.Z. Wang, Metall. Power, 5 (2006) 22–23.
[30] S. Yu, H.B. Zhao, S.S. Cheng and H.W. Pan, J. Iron Steel Res., 23 (2011) 20–27.
[31] E. Lectard, E. Hess and R. Lin, Rev. Metall., 101 (2004) 31–38.
[32] C.C. Lan, S.H. Zhang, B.Q. Wu, Q. Lyu and Y.Q. Sun, J. Iron Steel Res., 27 (2015) 1–8.